SUPPORTING INFORMATION

Spectroscopic and Polarization-Dependent Single-Molecule Tracking Reveal the One-Dimensional Diffusion Pathways in Surfactant-Templated Mesoporous Silica

Ruwandi Kumarasinghe, Eric D. Higgins, Takashi Ito and Daniel A. Higgins**

Department of Chemistry, Kansas State University, 213 CBC Building, Manhattan, Kansas 66506-0401, United States

The quantum mechanical modeling of NR is described, as are Monte Carlo simulations of its orientation within a model silica pore. A description of the procedures used to separate single molecules into immobile and mobile populations and those exhibiting 1D and 2D diffusion are also provided, as are representative MSD plots used in NR diffusion coefficient determinations. The procedure used to determine the NR octanol-water partition coefficient is also given. Finally, representative video data are included.

Quantum Mechanical Calculations

Electronic structure calculations were performed on Nile Red (NR) to determine the orientation of the transition dipole moment for its lowest energy electronic transition. The GAMESS software package was employed for optimizing the structure and modeling the electronic properties of NR.[1] NR was first constructed and its structure initially optimized using the Avogadro software package.[2] Its structure was then fully optimized in GAMESS at the Hartree-Fock level, using the 6-31G basis set. The electronic orbitals were also obtained at the same level of theory. The electronic transitions were obtained from a full configuration interaction using the graphical unitary group approach at the single excitation level. Table S1 gives the parameters obtained for first four electronic transitions. Figure S1 displays the optimized NR structure and the HOMO, LUMO and LUMO+1 orbitals. The lowest energy electronic transition involves promotion of an electron from the HOMO to a combination of orbitals dominated by the LUMO and LUMO+1.

The ground and excited state dipole moments for NR were found to be 7.5 Debye and 12.5 Debye, respectively, values that compare favorably with previously-reported experimental and theoretical results.[3-5] The ~ 5 Debye increase in the dipole moment upon excitation of NR explains its strong sensitivity to solvent polarity.[6] The transition dipole associated with the lowest energy electronic transition was determined to deviate from the long axis of the molecule by ~ 7°. The long axis of NR was assigned by fitting the positions of all atoms to a line using orthogonal regression methods.[7-9]

Table S1. Electronic transitions of Nile Red obtained from GAMESS modeling using the 6-31G basis set.

Transition	Energy[a]	Wavelength[b]	Trans. Dipole[c]	Osc. Strength
1[d]	3.41	364	8.03	0.834
2	4.30	289	0.53	0.005
3	4.57	271	0.12	0.000
4	4.69	264	1.47	0.039

[a] Energy is given in eV, [b] wavelength is in nm and [c] transition dipoles in Debye. [d] The first transition represents the transition probed in the spectroscopic and single-molecule experiments.

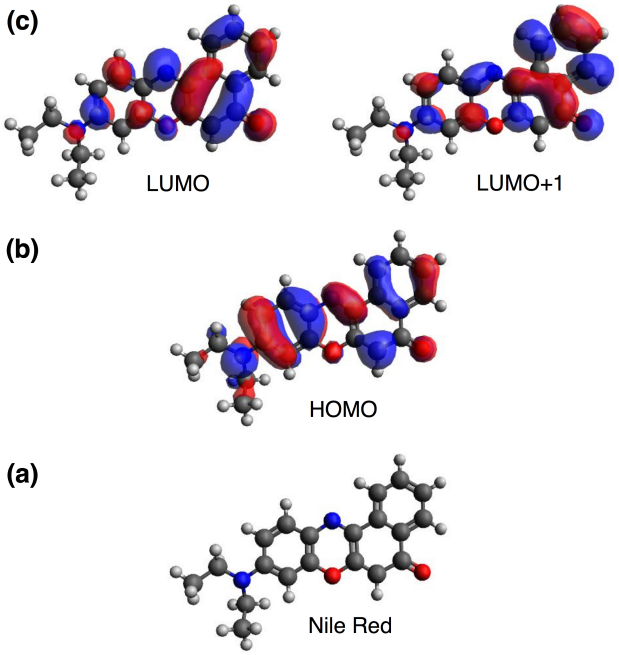

Figure S1. **(a)** Optimized geometry of the Nile Red molecule. **(b)** HOMO representation for Nile Red. **(c)** LUMO and LUMO+1 representations. The lowest energy electronic transition in Nile Red is characterized primarily as a HOMO to LUMO and LUMO+1 transition.

Assessing Molecular Mobility and Dimensionality of Motion

Separation of the trajectories into mobile and immobile populations and the former into 1D and 2D diffusing populations was accomplished by first estimating the localization precision for each molecule, using the method reported by Thompson, et al.[10] The amplitudes of the fitted

spots were used to determine the total number of photons detected from each spot. The standard deviation of the background counts, determined from regions where no molecules were found, was used to estimate the effective background count level. The calibrated pixel size in the videos was 125 nm, as determined from images of hexagonal arrays of 1 μm diameter fluorescent polystyrene beads. These parameters yielded common localization precisions, σ, of ~ 20 nm. Further analysis of the trajectory data was accomplished by previously-reported orthogonal regression methods.[11] Among other useful parameters, this analysis provides measures of the localization variance, σ_δ^2, averaged across each trajectory, and the motional variance, σ_R^2, due to molecular diffusion along a 1D pathway. Molecules having $\sigma_\delta^2 \leq 4.6\sigma^2$ were assigned to the immobile population, while all others were classified as mobile. Of the mobile molecules, those having $\sigma_R^2 \geq 4.6\sigma_\delta^2$ were classified as diffusing in 1D, while all others were classified as 2D diffusing molecules.

Diffusion Coefficient Determinations for NR Single Molecules

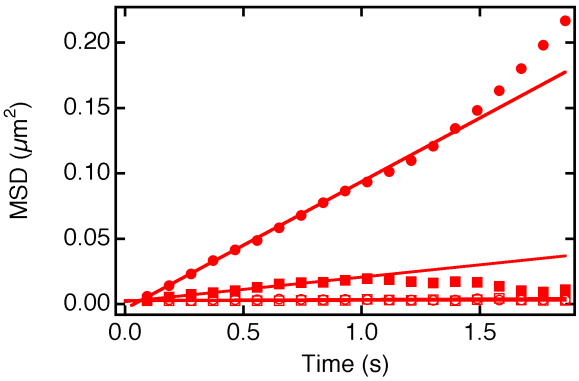

Figure S2. Plots of mean square displacement data (symbols) for the four single molecule trajectories shown in **Figure 4** (main text) and their fits (straight lines). The filled circles and squares show data from **Figure 4a,b** while the open circles and squares show data from **Figure 4c,d**. Each data set is plotted out to a 20 frame (~ 1.9 s) delay.

Partition Coefficient Measurements

The octanol-water partition coefficient for NR was determined by filling a 125 mL separatory funnel with a 25 mL aliquot of 2.5 μM NR solution in *n*-octanol and 25 mL of deionized water. The solution was then vigorously shaken for ~ 5 min, after which the solutions were allowed to separate for a period of 1.5 h. The water was then drained, a second aliquot of water added and the extraction repeated. A total of 5 extractions were performed with fresh volumes of water. After the final extraction, the octanol was drained from the separatory funnel and the absorbance of NR was measured in a 1 cm pathlength cuvette at 535 nm. All procedures were performed at ~ 23 °C.

Monte Carlo Simulations

Simulations of the orientation distribution expected for NR within an empty 3.5 nm diameter model silica pore were performed using software written in house.[12] In these simulations, random central positions and orientations were generated for each molecule within the pore. The pairwise interaction energies between the NR atoms and those of the pore were then determined using a Lennard-Jones potential. The σ and ε values employed to define the interaction distances and energies are given in Tables S2, S3. The Lennard-Jones parameters used for interactions between pairs of different atoms were obtained using the Lorentz-Berthelot combining rules.[13] The Metropolis Algorithm[12] was employed to accept or reject each molecular configuration within the pore, using a temperature of 298K. Convergence of the results was verified by repeating the simulations multiple times for varying numbers of attempts up to $3x10^5$.

Table S2. Lennard-Jones parameters for all pore atoms.[14]

Atom	σ (Angs)	ε (kcal/mol)
Si	2.500	0.0001
O	2.700	0.4569
H(OH)	1.295	0.0004
O(OH)	3.070	0.1700

Table S3. Lennard-Jones parameters for all NR atoms.[14]

Atom	σ (Angs)	ε (kcal/mol)
C	3.400	0.086
H	2.650	0.015
N	3.250	0.170
O	2.960	0.210

Video S1. Two-color single-molecule fluorescence video data acquired from an NR doped surfactant- and solvent-filled mesoporous silica film. The left half of the video shows data acquired in a spectral band centered at ~625 nm while the right half shows data acquired in a band centered at ~ 580 nm. This video is also shown in Figure 3 of the main text as a Z-projection image.

Video S2. Two-polarization single-molecule fluorescence video data acquired from an NR doped surfactant- and solvent-filled mesoporous silica film. The left half of the video shows data acquired for light polarized in the horizontal direction on the image plane while the right half shows data acquired for light polarized in the vertical direction. This video is also shown in Figure 6 of the main text as a Z-projection image.

REFERENCES

(1) Schmidt, M. W.; Baldridge, K. K.; Boatz, J. A.; Elbert, S. T.; Gordon, M. S.; Jensen, J. H.; Koseki, S.; Matsunaga, N.; Nguyen, K. A.; Su, S. J.; et al. General Atomic and Molecular Electronic Structure System. *J. Comput. Chem.* **1993**, *14*, 1347-1363.

(2) Hanwell, M. D.; Curtis, D. E.; Lonie, D. C.; Vandermeersch, T.; Zurek, E.; Hutchison, G. R. Avogadro: An Advanced Semantic Chemical Editor, Visualization and Analysis Platform. *J. Cheminformatics* **2012**, *4*, 1-17.

(3) Dutt, G. B.; Doraiswamy, S.; Periasamy, N. Molecular Reorientation Dynamics of Polar Dye Probes in Tertiary-Butyl Alcohol-Water Mixtures. *J. Chem. Phys.* **1991**, *94*, 5360-5368.

(4) Sarkar, N.; Das, K.; Nath, D. N.; Bhattacharyya, K. Twisted Charge Transfer Process of Nile Red in Homogeneous Solution and in Fauhasite Zeolite. *Langmuir* **1994**, *10*, 326-329.

(5) Dutta, A. K.; Kamada, K.; Ohta, K. Spectroscopic Studies of Nile Red in Organic Solvents and Polymers. *J. Photochem. Photobiol. A* **1996**, *93*, 57-64.

(6) Deye, J. F.; Berger, T. A.; Anderson, A. G. Nile Red as a Solvatochromic Dye for Measruing Solvent Strength in Normal Liquids and Mixtures of Normal Liquids with Supercritical and Near Critical Fluids. *Anal. Chem.* **1990**, *62*, 615-622.

(7) Adcock, R. J. A Problem in Least Squares. *The Analyst* **1878**, *5*, 53-54.

(8) Deming, W. E.: *Statistical Adjustment of Data*; Wiley: New York, 1943.

(9) Dunn, G.: *Statistical Evaluation of Measurement Errors: Design and Analysis of Reliability Studies*; Arnold: London, 2004.

(10) Thompson, R. E.; Larson, D. R.; Webb, W. W. Precise Nanometer Localization Analysis for Individual Fluorescent Probes. *Biophys. J.* **2002**, *82*, 2775-2783.

(11) Tran Ba, K. H.; Everett, T. A.; Ito, T.; Higgins, D. A. Trajectory Angle Determination in One Dimensional Single Molecule Tracking Data by Orthogonal Regression Analysis. *Phys. Chem. Chem. Phys.* **2011**, *13*, 1827-1835.

(12) Frenkel, D.; Smit, B.: *Understanding Molecular Simulation: From Algorithms to Applications*; Academic Press: San Diego, 1996.

(13) Bernreuther, M.; Buchholz, M.; Bungartz, H.-J.: Aspects of a Parallel Molecular Dynamics Software for Nano-FLuidics. In *Parallel Comuting: Architectures, Algorithms and Applications*; Bischof, C., Brückner, M., Gibbon, P., Joubert, G. R., Lippert, T., Mohr, B., Peteres, F., Eds.; IOS Press: Amsterdam, 2008; pp 53-60.

(14) Harvey, J. A.; Thompson, W. H. Thermodynamic Driving Forces for Dye Molecule Position and Orientation in Nanoconfined Solvents. *J. Phys. Chem. B* **2015**, *119*, 9150-9159.